Dielectric Properties of Nanocomposites Based on Polystyrene and Polyhedral Oligomeric Phenethyl-Silsesquioxanes

Ning Hao, Martin Böhning, and Andreas Schönhals*

Federal Institute of Materials Research and Testing (BAM) Unter den Eichen 87, D-12205 Berlin, Germany

Received August 7, 2007; Revised Manuscript Received October 19, 2007

ABSTRACT: Nanocomposites were prepared by solution blending of polyhedral oligomeric silsesquioxane with phenethyl substituents (PhenethylPOSS) into polystyrene (PS). The prepared materials were investigated by dielectric spectroscopy, differential scanning calorimetry (DSC), and density measurements. Additional FTIR investigations were carried out. Pure polystyrene shows two relaxation processes, an intermediate β*-process at lower and the α-relaxation at higher temperatures, the latter corresponding to segmental dynamics (dynamic glass transition). The molecular assignment of the β*-process needs further investigation. PhenethylPOSS can be incorporated into PS up to about 40 wt % without any indication of phase separation. With increasing PhenethylPOSS content, the α-relaxation of the composites shifts to lower temperatures and the loss peak broadens. Thus, the main effect of the nanofiller in the polystyrene matrix is to enhance the segmental dynamics, i.e., plasticization. The incorporation of approximately 40 wt % (approximately 5 mol %) PhenethylPOSS shifts the glass transition temperature T_g by 50 K to lower temperatures. The obtained results for polystyrene are discussed together with those reported recently for polycarbonate where a phase-separated morphology is observed for higher concentrations of PhenethylPOSS. The different behavior of PhenethylPOSS in polystyrene and polycarbonate is interpreted in terms of the different interaction of the phenyl rings within the POSS substituents with the phenyl rings of the polymers. For polystyrene, the interaction is stronger than for polycarbonate which probably leads to the enhanced miscibility of PhenethylPOSS into polystyrene. A detailed analysis of the temperature dependence of the dielectric relaxation strengths points also to additional interactions in the nanocomposites when compared to pure polystyrene. The broadening of the loss peak with increasing concentration is discussed in the framework of composition fluctuations.

1. Introduction

Hybrid materials based on polymers with nanoscaled inorganic fillers become more and more important in conventional engineering but also for various high-tech applications for instance in microelectronics, optics, etc. (see for instance refs 1−7). The property improvement of such polymer based nanocomposites compared to conventional scaled composites is a direct consequence of the size of the incorporated particles in the nanometer range. In addition to that, the role of the interfacial area between the nanoparticles and the polymer matrix is important which includes also the interaction of the nanoparticle with the segments of the polymer chains. Because of the high surface to volume ratio of the nanoparticles, the volume fraction of this interfacial area is high.[1−3]

Recently, polyhedral oligomeric silsesquioxanes (POSS[8]) has been increasingly used as nanofiller (see for instance refs 9−12). POSS itself is a hybrid organic−inorganic structure. It consists of a silica cage in the core with organic substituents R attached at the edges of the cage. The general formula of it is $(SiO_{1.5})_nR_n$[10] where n is the number of silicon atoms of the inner cage (n = 8,10,12...). From the chemical point of view, POSS is a complex molecule but it can be regarded more general as the smallest possible silica particle surrounded by an organic surface.[10,13] Because of the fact that a broad variety of substituents can be attached to the silica core, the compatibility between a "POSS nanoparticle" and different polymeric matrixes can be tuned.

The chemistry of POSS is quite flexible. By introduction of polymerizable functional groups in the substituents, POSS can be incorporated into polymer chains or act as a crosslinker.[14] Compared to the incorporation of POSS by chemical bonding, blending is a simple and inexpensive way to obtain polymer-based nanocomposites. Recently, POSS with different substituents have been blended into a variety of commercial polymers[14] such as polypropylene,[15−19] high-density polyethylene (HDPE),[20,21] poly(methyl methacrylate) (PMMA),[22−25] poly(vinyl chloride),[26,27] poly(ethylene terephthalate),[28−30] polystyrene,[31−34] poly(vinyl ester resin),[35] and poly(bisphenol A carbonate) (PBAC).[11,12] An improvement of the material characteristics of POSS containing nanocomposites, including the enhancement of the thermal stability and the mechanical properties, has been reported for different systems. Moreover it was also found that the glass transition temperature (T_g) of the nanocomposites depends on the substituents and the concentration of the POSS compound. This was reported for instance for PMMA,[24,25] poly(vinyl chloride),[26,27] and also for polycarbonate.[12]

One problem of the blending method is to maintain a stable dispersion of the POSS molecules in the polymer matrix on a molecular level even for higher concentrations of POSS. For instance it was found for isobutylPOSS/PMMA,[25] octamethylPOSS/HDPE,[21] and phenethylPOSS/PBAC[12] that POSS can be only dispersed in the matrix on a molecular level up to a critical concentration $c_{critical}$. For higher concentrations than that, phase separated morphologies are observed. The absolute value of $c_{critical}$ depends on the interaction between the substituents R and the repeat units of the polymer chain. Therefore adjusting the interaction of the POSS substituents may enhance the compatibility of the filler and the polymer matrix. This was

* Corresponding author. A. Schoenhals, Federal Institute for Materials Research and Testing (BAM VI.5), Unter den Eichen 87, D-12200 Berlin, Germany. Telephone +49 30/8104-3384; fax +49 30/8104-1637. E-mail: Andreas.Schoenhals@bam.de.

10.1021/ma071777g CCC: $37.00
Published on Web 12/04/2007

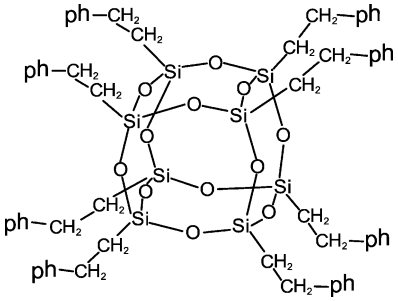

Figure 1. Chemical structure of octa-PhenethylPOSS (ph = phenyl).

proved for blending isooctylPOSS into isotactic polypropylene.[36] Because of the long alkyl substituents, POSS could be well dispersed into PP. Also for phenethylPOSS/PS nanocomposites it was found that due to the interaction of the phenyl rings of the nanofiller with those of the matrix, POSS can be molecularly dispersed into polystyrene up to about 20 wt %.[37]

Recently, we employed dielectric spectroscopy to study the structure property relationships of nanocomposites based on polycarbonate and POSS with phenethyl substituents (PhenethylPOSS[8]).[12] As a main result it was found that PhenethylPOSS can be dispersed on a molecular level up to approximately 7 wt % in the polycarbonate matrix and acts as a plasticizer. For higher concentrations of PhenethylPOSS, a phase separated morphology is found consisting of a polycarbonate rich matrix with molecularly dispersed POSS and POSS-rich domains. These domains are surrounded by an interfacial layer of polycarbonate having a higher concentration of PhenethylPOSS then the remaining matrix.[12] In the continuation of that work here, polystyrene is used as the matrix polymer where PhenethylPOSS is again used as the nanofiller. The same conditions were applied to prepare the nanocomposites. The obtained results will be compared with those obtained for the PhenethylPOSS/polycarbonate system. For melt blending, it was found by Blanski et al. that PhenethylPOSS can be incorporated into polystyrene up to 20% on a molecular level.[37]

2. Experimental Section

2.1. Materials and Sample Preparation. Polystyrene (PS) was purchased from Sigma-Aldrich and used as the matrix polymer (M_n = 985 000 g/mol, polydispersity index (PDI) = 2.02). PhenethylPOSS was purchased from Hybridplastics Inc. Its molecular structure is given in Figure 1. The composition of the obtained product was discussed in detail in ref 12. MALDI-TOF mass spectrometry showed that it consists of a mixture of octa-PhenethylPOSS (n = 8, T8-cage), deca-PhenethylPOSS (n = 10, T10-cage), dodeca-PhenethylPOSS (n = 12, T12-cage), and probably smaller amounts of POSS of higher cage sizes. Both the polystyrene as well as the POSS were used without further purification.

The route for the preparation of the nanocomposites is given in detail in ref 12. Here, polystyrene is solvated in chloroform (15 wt %, solvent reagent grade). PhenethylPOSS was dispersed in that solution with the selected concentrations. Ultrasonification (Bandelin Sonopuls, HD200/UW200 homogenizer equipped with KE76 titanium tapered tip) was applied for at least 5 min to stabilize this mixture. A custom-made casting knife was used to cast the solution onto a polished glass substrate. To control the initial evaporation of the solvent from the film, the glass plate was placed in a closed chamber. After that initial step, the films were removed from the substrate and heated in vacuum up to 343 K. At this temperature, the sample was annealed for 24 h to remove the residual solvent. The selected annealing temperature is below the glass transition temperature of PS. The temperature was chosen because also gas transport measurements were carried out on the same set of nanocomposites. For these measurements, pinhole free samples with plane surfaces (35 mm in diameter) are required. Such samples cannot be obtained by annealing the film above its glass transition temperature. The results of the gas transport measurements are published elsewhere[38] together with a comparison of the dielectric data given here. Thermogravimetry (TGA) was applied to check the complete removal of the solvent. Furthermore the glass transition temperature measured for a solution prepared film agrees with literature data given for bulk PS. With the use of this procedure, flat and transparent samples can be prepared up to 40 wt % of POSS. With an increasing concentration of PhenethylPOSS, the films become more and more brittle. Above 40 wt % of POSS, no stable films could be obtained anymore. Details of the prepared samples are listed in Table 1. The last digits in the sample codes represent the nominal weight fraction of PhenethylPOSS. All concentrations given within the paper and also in the figure captions are calculated from the formulation.

Table 1. Composition and Codes of the Investigated Nanocomposites, All Compositions Were Calculated from the Formulation (In Addition, Glass Transition Temperatures Estimated by DSC and Densities Are Given)

sample code	c_{POSS} [wt %]	x_{POSS} [mol %]	T_g [K]	ρ [g/cm^3]
PS000	0	0	373.1	1.045
PS005	4.7	0.5	362.3	1.062
PS010	9.1	1.0	358.0	1.072
PS013	13.1	1.4	355.9	1.077
PS022	22.1	2.6	351.7	1.082
PS032	31.9	4.3	343.0	1.101
PS038	38.3	5.5	325.8	1.126
PhenethylPOSS	100	100	243.7	1.215

2.2. Methods. To check the concentration of PhenethylPOSS in the prepared nanocomposites, FTIR was employed. The infrared spectra of the samples were measured using a Thermo-Nicolet (Nexus 670) FTIR spectrometer at room temperature. The nanocomposites were measured in transmission, while the IR spectrum of pure PhenethylPOSS was measured by attenuated total reflection-IR (ATR-IR). For all samples, the spectra were taken in the wavenumber range from 400 to 4000 cm^{-1}. During the measurements, 64 scans with a resolution of 2 cm^{-1} were recorded.

The structure property relationships of the prepared nanocomposites were studied by dielectric spectroscopy, thermal analysis, and density measurements. Dielectric spectroscopy is sensitive to molecular fluctuations of dipoles within the system which can be taken as a probe for structure. For details see ref 39. A high-resolution ALPHA analyzer (Novocontrol) is used to measure the complex dielectric function $\epsilon^*(f) = \epsilon'(f) - i\epsilon''(f)$ in parallel plate geometry (f, frequency; ϵ' and ϵ'', real and imaginary part of the complex dielectric function, $i = \sqrt{-1}$). The sample was placed between two gold-covered stainless steel electrodes and isothermally measured in the frequency range from 10^{-1} Hz to 10^7 Hz. Its temperature was controlled by a Quatro Novocontrol cryo-system with a temperature stability better than 0.1 K. For more details see ref 40.

Thermal analysis was carried out by differential scanning calorimetry (DSC, Seiko). The samples were measured in the temperature range from 173 to 473 K with a rate of 10 K/min. N_2 was used as the protection gas. The glass transition temperature T_g was taken as the inflection point of the heat flow of the second heating run. (The difference in the glass transition temperatures of the first and second heating run was typically 1−2 K). The measured T_g values of the samples are listed in Table 1.

A density gradient column (DGC) was employed to measure the density of the samples according to DIN 53479 at the required temperature of 296.15 K (23 °C, temperature error 0.3 K). In order to measure densities from 1.175 to 1.220 g/cm^3, solutions of isopropanol with distilled water were employed. The density of the sample is determined by polynomial interpolation between that of glass floats having well-defined values. Density values were taken each day during one week after the calibration of the DGC and average densities were calculated. The error of these subsequent

measurements is below 1%. The first value of the density was taken 24 h after the insertion of the sample into the DGC. The absolute error in the calibration of the glass floats is below 2%.

3. Results and Discussions

The structure of the paper is organized as follows. First the dielectric properties of the PhenethylPOSS/PS nanocomposites are discussed. In the second part a detailed comparison with that of PhenethylPOSS/PBAC is presented.

PhenethylPOSS/Polystyrene Nanocomposites. Infrared spectroscopy was applied to determine the content of PhenethylPOSS in the nanocomposites. The IR spectra of the pure PS, PhenethylPOSS, and a nanocomposite with 22.1 wt % POSS are shown in Figure 2.

The *y*-scale is different for pure POSS and the nanocomposites because the former is measured using the ATR technique. A series of characteristic absorption peaks can be identified from the spectra.[41,42] The broad peak around 3000 cm^{-1} is due to the vibration of the C−H bonds of the phenyl rings, while the double-peak-structure at 1452 and 1496 cm^{-1} is assigned to the CH_2 groups. A broad absorption peak around 1078 cm^{-1} is observed for bulk PhenethylPOSS which is due to the vibrations of the −Si−O−Si− bond of POSS. Blending POSS molecules into PS slightly shifts this band to higher wavenumbers (1103 cm^{-1}). It increases in intensity with increasing concentration of POSS. Thus, the band at 1103 cm^{-1} is used to characterize the content of POSS in the nanocomposites. The quantitative IR-analysis of PS-based PhenethylPOSS nanocomposites is difficult because all of the characteristic bands of PS overlap with bands of the bulk PhenethylPOSS. Therefore advantage is taken from the fact that although the weight fraction of POSS is high, its molar fraction x_{POSS} is low (see Table 1). This means the number of POSS molecules is small compared to the number of repeat units of polystyrene. Therefore it is assumed that the contribution of the phenyl rings of POSS to the band at 3000 cm^{-1} can be neglected and it can be taken as characteristic for polystyrene. After subtraction of the baseline, the intensity of the bands at 1103 and 3000 cm^{-1} is estimated by fitting a Gaussian to the data. The ratio of the intensities of theses bands I_{1103}/I_{3000} is plotted versus the mole fraction of PhenethylPOSS in the solution in Figure 3. This ratio scales linearly with x_{POSS} which can be described by

$$\left(\frac{I_{1103}}{I_{3000}}\right) = 1.7x_{POSS} \qquad (1)$$

This linear relationship proves that the molar concentration of the POSS in nanocomposites is equal to that of the formulation.

The dielectric behavior of pure PhenethylPOSS is discussed in detail in ref 12. One dielectrically active relaxation process is observed which corresponds to the dynamic glass transition (α-relaxation) of PhenethylPOSS. This was supported by DSC measurements.

Polystyrene has a weak dipole moment, and therefore the dielectric loss is low. At least one relaxation region indicated by a peak in ϵ'' could be identified. It is assigned to the α-relaxation of polystyrene due to segmental fluctuations. A closer inspection of the spectra reveals that there is a weak shoulder at the low-temperature side of the α-process which corresponds to a second relaxation process (β*). Also Wübbenhorst et al. discussed, besides the dynamic glass transition, additional relaxation processes for PS which where assigned on a molecular level to fluctuations of helices or parts of it.[43,44] The molecular origin of the β*-process is unclear up to now and needs further investigation. Although, it should be noted

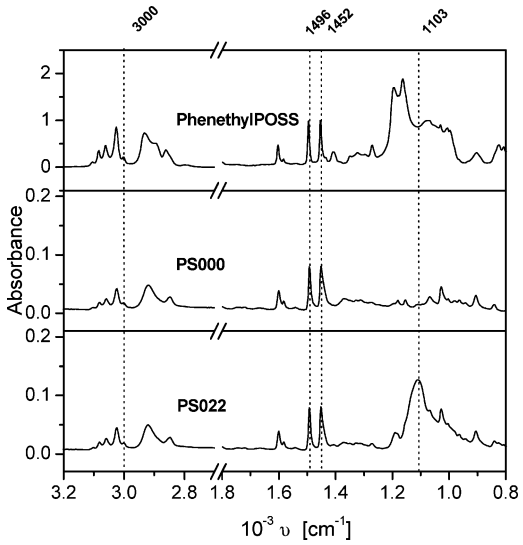

Figure 2. IR spectra of PhenethylPOSS, polystyrene, and a PS-based nanocomposite with 22.1 wt % POSS (PS022). The concentration was calculated from the formulation.

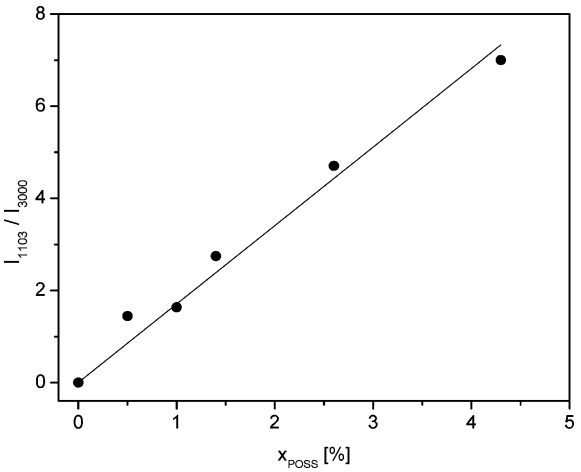

Figure 3. Ratio of the FTIR intensities I_{1103}/I_{3000} vs molar fraction of POSS x_{POSS}. The line is a linear regression to the data.

that such an intermediate relaxation process was also observed for other polymers having phenyl rings in the repeat unit like polycarbonate,[12,45,46] poly(ethylene 2,6 naphthalene dicarboxylate),[47] or side-chain polymers based on polymethacrylate.[48,49] Therefore, it might be concluded that such an intermediate relaxation process is characteristic for polymers having phenyl rings in the structure. To be complete at low temperature might be some indication for a β-process, but the loss is too weak for a quantitative discussion.

The model function of Havriliak−Negami (HN-function)[50] is used to analyze the dielectric measurements quantitatively. It reads

$$\epsilon^*(f) - \epsilon_\infty = \frac{\Delta\epsilon}{(1 + (\mathrm{i}\, f/f_0)^\beta)^\gamma} \qquad (2)$$

f_0 is a characteristic frequency related to the frequency of maximal loss f_p (relaxation rate), ϵ_∞ describes the value of the real part ϵ' for $f \gg f_0$. β and γ are fractional parameters ($0 < \beta \leq 1$ and $0 < \beta\gamma \leq 1$) characterizing the shape of the relaxation time spectra. $\Delta\epsilon$ denotes the dielectric strength. From the fit of the HN-function to the data, the relaxation rate f_p, the dielectric strength, and the shape parameters are determined. Conduction effects are treated in the usual way by adding a contribution

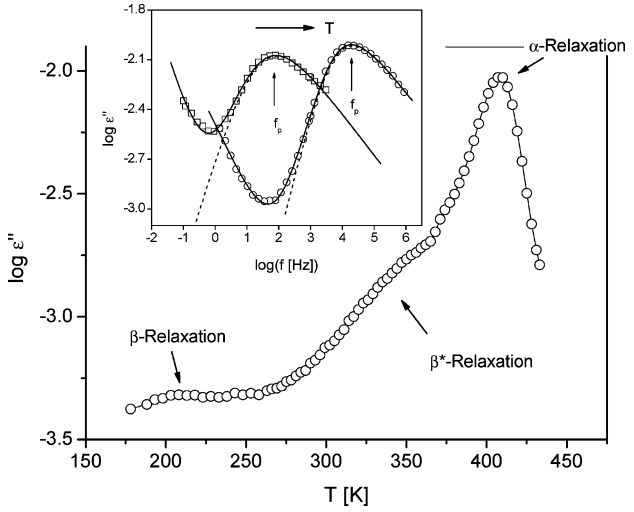

Figure 4. Dielectric loss vs temperature for pure PS at a frequency of 10 kHz. The line is a guide for the eyes. The inset gives the dielectric loss versus frequency for two different temperatures above T_g: □ — 389.7 K; ○ – 410.7 K. The — line is a fit of the HN-function to the data including a conductivity contribution. The - - - line gives the contribution of the relaxation process.

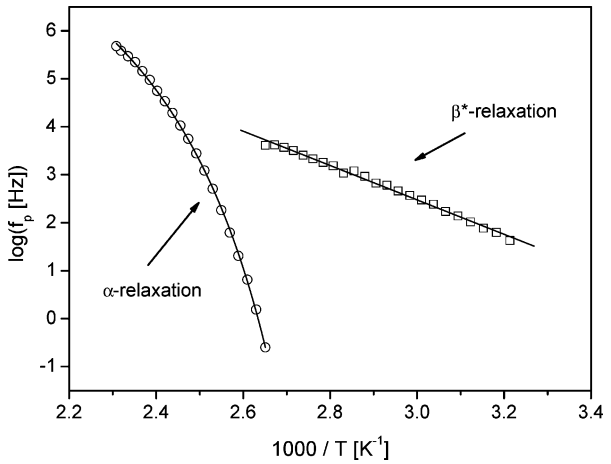

Figure 5. Relaxation rate f_p vs inverse temperature for the α-(○) and the β*-(□) relaxation. The lines are fits of the VFT-equation to the data of the α-relaxation and the Arrhenius equation to that of the β*-process.

$\sigma_0/[(2\pi f)^s\epsilon_0]$ to the dielectric loss where σ_0 is related to the specific dc conductivity of the sample and ϵ_0 is the dielectric permittivity of vacuum. The parameter s ($0 < s \leq 1$) describes for $s = 1$ Ohmic and for $s < 1$ non-Ohmic effects in the conductivity. For details see ref 51.

Some examples of fitting the HN-equation to the α- relaxation are given in the inset of Figure 4. The relaxation rates f_p of both processes are plotted versus reciprocal temperature in Figure 5. f_p for the α-relaxation can be well described by the Vogel−Fulcher−Tammann- (VFT-) equation[52] which reads

$$\log f_p = \log f_\infty - \frac{A}{T - T_0} \tag{3}$$

(log f_∞ and A are constants, T_0 is the so-called Vogel temperature). All fit parameters are given in Table 2. For the β*-relaxation, the data follows the Arrhenius law

$$f_p = f_\infty \exp\left(-\frac{E_A}{k_B T}\right) \tag{4}$$

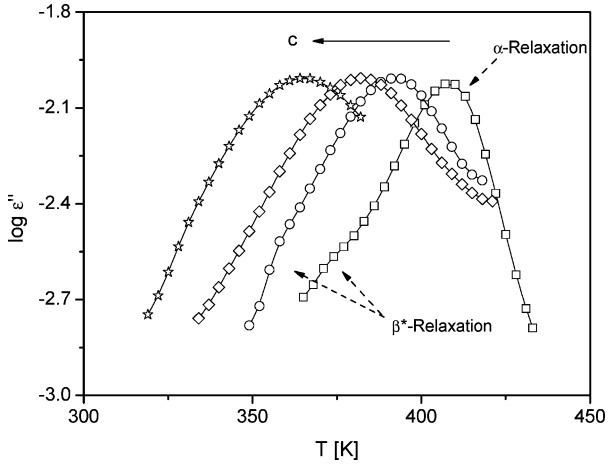

Figure 6. Dielectric loss vs temperature at a frequency of 10 kHz for pure PS (□) and different nanocomposites: ○, PS010; ◇, PS032; ☆, PS038. Lines are guides for the eyes.

Table 2. Estimated VFT Parameters

	α-relaxation		
sample code	log(f_∞ [Hz])	A [K]	T_0 [K]
PhenethylPOSS	11.4	334	218.2
PS000	10.5	475.3	334.4
PS005	10.8	455.4	333.0
PS010	10.8	454.7	325.8
PS013	10.5	371.9	334.7
PS022	10.5	481.5	314.9
PS033	10.0	433.0	306.5
PS038	10.0	438.1	290.0

where k_B is Boltzmann's constant. For the activation energy, E_A, a value of 68.5 kJ/mol is estimated and the pre-exponential factor, f_∞, is log(f_∞ [Hz]) = 13.2. It should be noted that E_A and the pre-exponential factor correspond to the values found by Wübbenhorst et al.[43] for the β_1-process.

Figure 6 gives the dielectric loss versus temperature for several nanocomposites at a fixed frequency of 10 kHz. Compared to pure PS for the composites, the α-relaxation shifts to lower temperatures with increasing concentration of POSS. This is in agreement with the corresponding DSC measurements. In addition, the loss peak broadens, but up to the highest concentrations of PhenethylPOSS there is no sign of a double peak structure as it is observed for PhenethylPOSS/polycarbonate nanocomposites.[12] Moreover in the temperature region of the glass transition of pure PhenethylPOSS, no additional relaxation process is found. This indicates that no phase separation takes place in the PhenethylPOSS/PS system up to the highest concentration of approximately 40 wt % of POSS. This is in agreement with results found by Blanski et al.[37] for PhenethylPOSS/PS with about 20 wt % of POSS by TEM.

In addition to Figure 6, Figure 7 compares the dielectric loss versus frequency for pure polystyrene and two nanocomposites at the same temperature. Adding 38 wt % PhenethylPOSS shifts the α-relaxation by about six decades to higher frequencies. This increase in molecular mobility (or decreased glass transition temperature) is known as plasticization. A similar behavior is also reported for nanocomposites prepared from PMMA and POSS with acrylic, cyclohexyl, and isobutyl substituents,[24,25] for a system based on poly(vinyl chloride) and MethacrylPOSS[27] and PhenethylPOSS/PBAC[12] nanocomposites as well.

The relaxation rates f_p of the nanocomposites were estimated by fitting the HN-function to the data (see Figure 7) and plotted versus reciprocal temperature in Figure 8. As seen already from the raw data, the curves shift to lower temperatures with

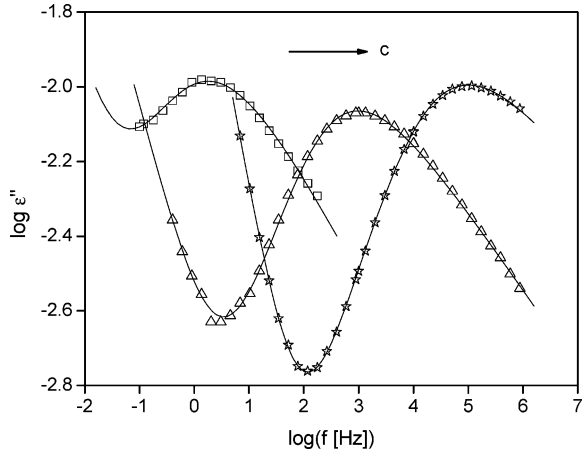

Figure 7. Dielectric loss vs frequency at a temperature of $T = 380.2$ K for pure PS (□) and different nanocomposites: △, PS022; ☆, PS038. Lines are fits of the HN-function to the data including a conductivity contribution.

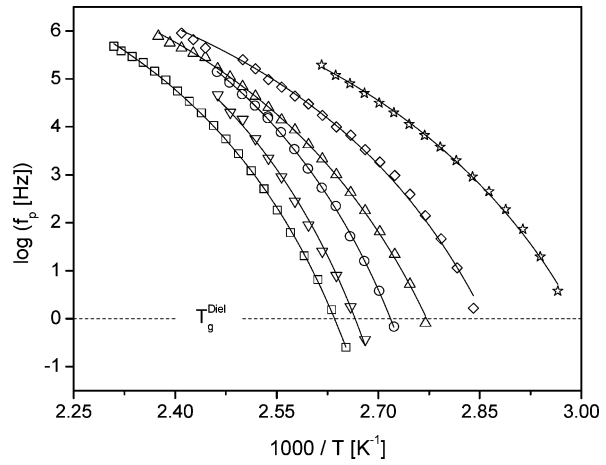

Figure 8. Relaxation rate f_p vs inverse temperature for the α-relaxation of the PhenethylPOSS/PS nanocomposites: □, PS; ▽, PS005; ○, PS010, △, PS022; ◇, PS032; ☆, PS038. The data for PS013 are not shown for sake of clearness. The lines are fits of the VFT-equation to the data.

increasing concentration of PhenethylPOSS. The data are analyzed by fitting the VFT-equation to it. A dielectric glass transition temperature $T_g^{Diel} = T(f_p = 1\ \text{Hz})$ can be estimated from that fit. The VFT-parameters are summarized in Table 2.

A closer inspection of the temperature dependence of the relaxation rates gives some indication that for higher concentrations of POSS the dependence is more complex than predicted by the VFT-equation. For a more detailed analysis of the temperature dependence of the relaxation rates, a derivative method is used.[53] This method is sensitive to the functional form of $f_p(T)$ irrespective of the prefactor. For a dependency according to the VFT-equation, one gets

$$\left[\frac{\mathrm{d}(\log f_p)}{\mathrm{d}T}\right]^{-1/2} = A^{-1/2}(T - T_0) \qquad (5)$$

In a plot $[\mathrm{d}(\log f_p)/\mathrm{d}T]^{-1/2}$ versus T, a VFT-behavior shows up as a straight line. This analysis shows (Figure 9) that indeed $f_p(T)$ for higher concentrations of PhenethylPOSS has two different temperature dependencies which can be described by two different VFT-equations, where polystyrene exhibits only a single VFT-dependence of the relaxation rates. The inset of Figure 9 provides the same analysis for pure PhenethylPOSS. The temperature dependence of the relaxation rates for pure POSS also shows a low and a high-temperature branch.

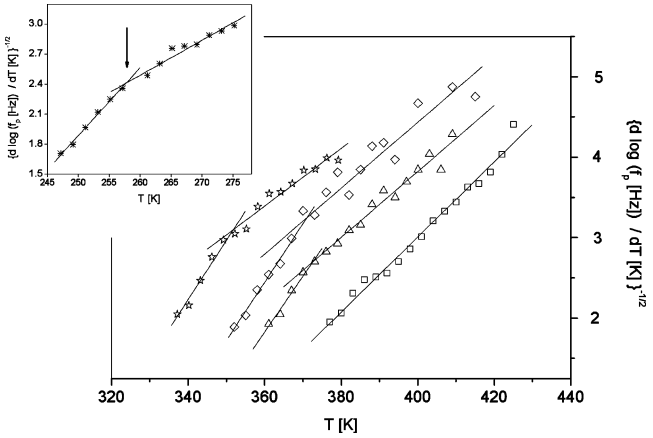

Figure 9. $[(\mathrm{d}(\log f_p))/(\mathrm{d}T)]^{-1/2}$ vs temperature for polystyrene (□) and different nanocomposites: △, PS022; ◇, PS032; ☆, PS038. The lines are linear regression to the low- and high-temperature branches of the data. The inset shows $[(\mathrm{d}(\log f_p))/(\mathrm{d}T)]^{-1/2}$ vs temperature for pure PhenethylPOSS. Like in the main figure, the lines are linear regression to the low- and high-temperature branches of the data.

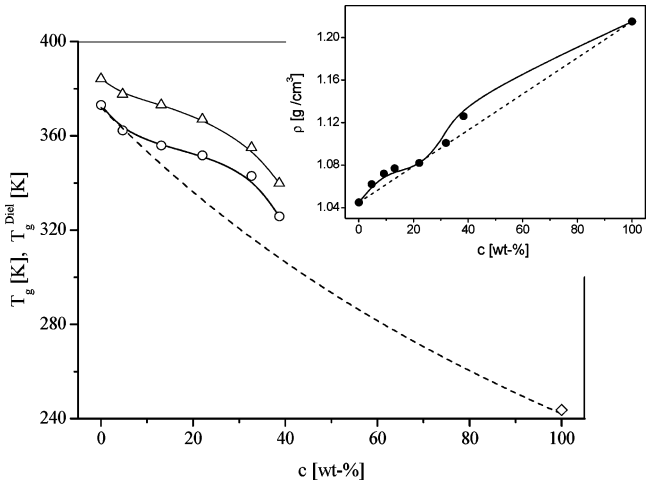

Figure 10. Dependence of the thermal glass transition temperature T_g and the dielectric glass transition temperature T_g^{Diel} on the concentration of PhenethylPOSS: ○, T_g; △, T_g^{Diel}. The — lines are guides for the eyes. The - - - line is the expectation from the Fox equation using the thermal glass transition temperature. ◇ gives the thermal glass transition temperature for pure PhenethylPOSS. The inset gives the density of the nanocomposites vs concentration. The — line is a guide for the eyes. The - - - line may characterize a simple additive behavior.

Therefore it is concluded that for higher concentrations of PhenethylPOSS in polystyrene, the molecular dynamics of the nanocomposite is controlled more and more by POSS.

The main effect of PhenethylPOSS in the nanocomposite is the acceleration of the segmental dynamics of the polystyrene matrix by plasticization. This is summarized by constructing a phase diagram. In Figure 10 both the thermal (T_g) and the dielectric glass transition temperature (T_g^{Diel}) is plotted versus the concentration of PhenethylPOSS. In addition the prediction of the Fox equation

$$\frac{1}{T_g} = \frac{c_{PS}}{T_{g,PS}} + \frac{c_{POSS}}{T_{g,POSS}} \qquad (c_{PS} + c_{POSS} = 1) \qquad (6)$$

is given which is expected to be valid for a blend which is miscible on a molecular level.

For all concentrations of POSS, both T_g and T_g^{Diel} decrease with increasing concentration of POSS but the values do not collapse into the line predicted by the Fox equation. Higher

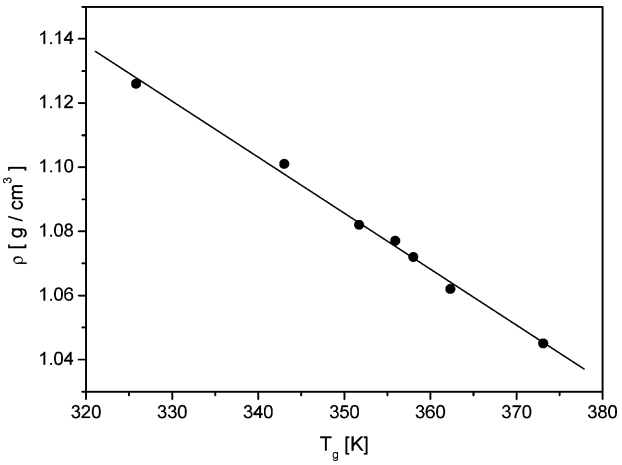

Figure 11. Density vs glass transition temperature. The line is a linear regression to the data.

values for the glass transition temperatures are observed for medium concentrations of PhenethylPOSS than expected from the Fox equation. For the highest concentration of POSS, the value approaches the Fox line again. This indicates extra effects taking place in the nanocomposite in addition to a simple mixing. This is also reflected by the concentration dependence of the density (see inset Figure 10). Again the data do not follow the line which should be characteristic for a simple additive system. On the other side, the glass transition temperature correlates linearly with the density of the system (see Figure 11). This indicates that the density is the controlling parameter.

The density and the glass transition temperature as well are higher than expected for a simple additive system. Both results point to the conjecture that an additional, preferential interaction is taking place in the nanocomposites. It is well-known that phenyl rings can form aggregates by a $\pi-\pi$ stacking interaction. Here it is assumed that the phenyl rings of POSS interact with those of polystyrene. This leads to a higher density than expected for an additive system In addition, the molecular mobility is slowed down and therefore the glass transition temperature is higher than expected as well. These preferential interactions enhance also the compatibility of POSS in polystyrene and are probably the reason that PhenethylPOSS can be blended into PS up to quite high concentrations.

Further evidence for preferential interaction in the nanocomposites is provided by the temperature dependence of the dielectric relaxation strength. The Debye theory of dielectric relaxation generalized by Kirkwood and Fröhlich[54] predicts the temperature dependence of the dielectric relaxation strength

$$\Delta\epsilon = \frac{1}{3\epsilon_0} g \frac{\mu^2}{k_B T} \frac{N}{V} = \frac{1}{3\epsilon_0} g \frac{\mu^2}{k_B T} \frac{\rho N_A}{M} \qquad (7)$$

where μ is the mean dipole moment related to the process under consideration and N/V is the number density of dipoles involved. g is the Kirkwood−Fröhlich correlation factor which describes static correlation between the dipoles. The Onsager factor describing internal field effects is omitted for sake of simplicity. The right-hand side of eq 7 is obtained by expressing the number density of dipoles by $\rho N_A M$ were M is the molar mass of the system and N_A denotes Avogadro's number.

In Figure 12 , $\Delta\epsilon$ for the α-relaxation is plotted versus inverse temperature for polystyrene, PhenethylPOSS, and several nanocomposites. Even for low concentrations of POSS, the slope of $\Delta\epsilon$ versus $1/T$ is much higher than that for polystyrene and similar to that of PhenethylPOSS. The net dipole moment of

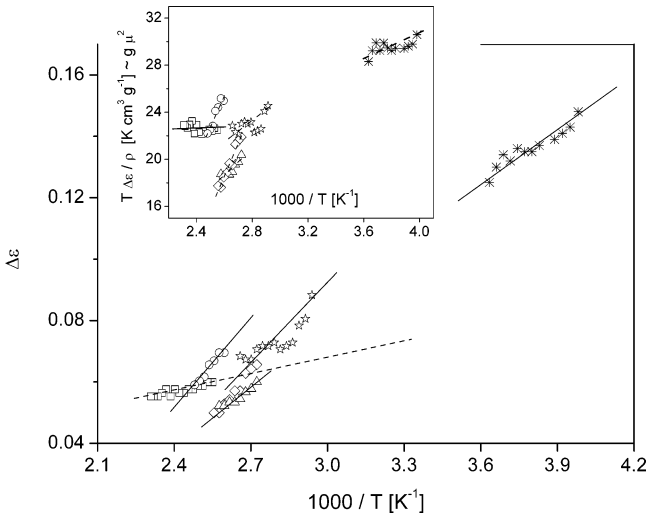

Figure 12. Dielectric strength $\Delta\epsilon$ vs inverse temperature: □, PS; ▽, PS005; ○, PS010; △, PS022; ◇, PS032; ☆, PS038; ∗, PhenethylPOSS. The lines are linear regressions to the data. The inset gives $T\Delta\epsilon/\rho \sim g\mu^2$ vs inverse temperature: □, PS; ▽, PS005; ○, PS010; △, PS022; ◇, PS032; ☆, PS038; ∗, PhenethylPOSS. The lines are linear regressions to the data.

the composite should be additive; this means that the Kirkwood−Fröhlich correlation factor g is increased for the nanocomposites in comparison to polystyrene. Because g describes static correlations between dipoles, it is concluded that the increased Kirkwood−Fröhlich factor reflects additional interactions. Because there are no other functional groups than the phenyl rings, it is assumed that these interactions are due to $\pi-\pi$ stacking. This becomes even more clear from the inset of Figure 12 where $T\Delta\epsilon/\rho \sim g\mu^2$ is plotted versus reciprocal temperature. For pure polystyrene, this quantity is independent of temperature, but for the nanocomposites and pure PhenethylPOSS, $T\Delta\epsilon/\rho \sim g\mu^2$ depends strongly on temperature. Because the dipole moment is independent of temperature, this result means that for nanocomposites the Kirkwood−Fröhlich factor and therefore the interactions give rise to temperature dependence: with increasing temperature, the interaction strength is decreasing.

To be complete, the change in the shape with increasing POSS concentration is also considered in the following. To compare the shape for the different composites, a normalization of the loss peak is necessary which can be done either by normalization using $\Delta\epsilon$ or the maximum height. The former is from a physical point more appropriate, but just to show that shape of the loss peak changes, the latter method can be chosen for simplicity. Figure 13 gives the dielectric loss normalized to it maximum value versus reduced frequency for different concentrations of PhenethylPOSS. Because the glass transition temperature depends strongly on the concentration, the dielectric spectra are taken at the temperature where the relaxation rate is 10^3 Hz to compare the different nanocomposites in the same dynamical state. With increasing POSS concentration, the loss peaks broadens mainly on the low-frequency side. To characterize the shape of the loss peak, the half-maximum height width (see Figure 13) is calculated from the HN-parameters.

In Figure 14, the half width is plotted versus the concentration of PhenethylPOSS. Again the temperature is taken where the relaxation of the sample is 10^3 Hz. As it can be seen already from the raw data, the half width increases with increasing POSS concentration. In the framework of recent theoretical approaches this can be understood by composition or concentration fluctuations.[55−58] Even when the distribution of POSS is

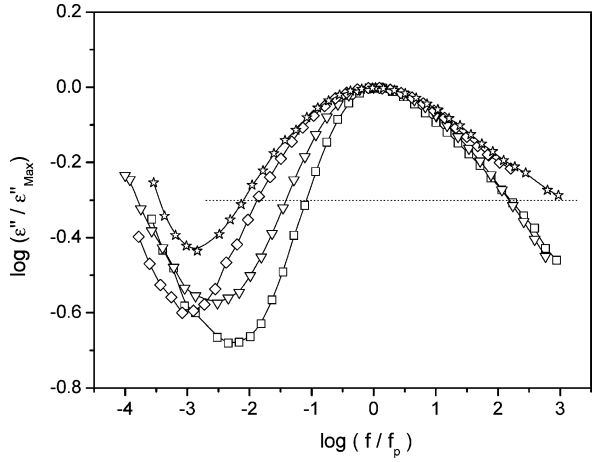

Figure 13. Reduced dielectric loss vs normalized frequency: □, PS ($T = 398.1$ K); ▽, PS005 ($T = 390.1$ K); ◇, PS032 ($T = 367.1$ K); ☆, PS038 ($T = 352.1$ K). The lines are guides for the eyes. The - - - line indicates the half-maximum height width.

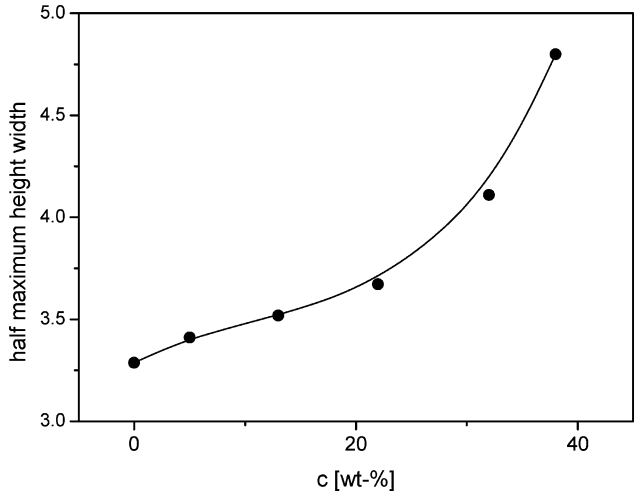

Figure 14. Half-maximum height width vs concentration of PhenethylPOSS at the temperature where the relaxation rate has a value of 10^3 Hz. (PS, $T = 398.1$; PS005, $T = 390.1$ K; PS013, $T = 384.1$ K; PS032, $T = 367.1$ K; PS038, $T = 352.1$ K). The maximum height width for pure PhenethylPOSS is 2.96 at $T = 261.1$ K which corresponds to the same value of the relaxation rate that is considered for the nanocomposites.

homogeneous on a macroscopic scale, it can fluctuate on a microscopic scale. In the cooperativity approaches to the glass transition[59,60] it is assumed that a cooperativity length scale of 2−3 nm is characteristic for glassy dynamics. It proposed that composition fluctuations in miscible polymer blends[57] and solvent/polymer systems[55,56] are taking place on this length scale. For these reasons, it is concluded that also for the investigated nanocomposites the broadening of the spectra is due to composition fluctuations of POSS in the range of a few nanometers. The dynamics of these composition fluctuations should be longer than the relaxations times of the dynamic glass transition.

Comparison of Polystyrene and Polycarbonate Nanocomposites. The main difference between polystyrene and polycarbonate based nanocomposites with PhenethylPOSS as the nanofiller is that the latter system undergoes a phase separation at a definite concentration of PhenethylPOSS while the former system remains miscible up to 40 wt % of PhenethylPOSS. The behavior of both systems is compared in a combined phase diagram (Figure 15) where the relative change of the glass transition temperature is plotted versus the concentration of POSS.

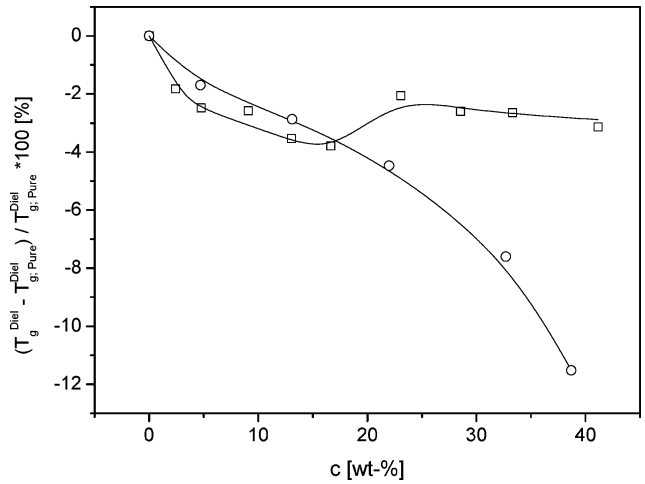

Figure 15. Relative dielectric glass transition temperature versus the concentration of PhenethylPOSS: ○, PS; □, polycarbonate. The lines are guides for the eyes.

For a low concentration of PhenethylPOSS, the dependence of the dynamic glass transition on it seems to be similar for both polymers. The values for polycarbonate are a little bit lower than that for polystyrene. To prove whether these differences are significant or not, additional experiments are necessary. At higher concentrations of POSS for PS, T_g^{Diel} decreases continuously where that for PBAC levels off due to phase separation and the fact that PhenethylPOSS can be solved only to a limited concentration of approximately 7 wt % on a molecular level into polycarbonate. The different miscibility behavior of PhenethylPOSS into polycarbonate and polystyrene might be attributed to the different interaction of the phenyl rings of POSS with the phenyl rings in the polymers. For PBAC, the phenyl ring is part of the main chain where for PS it is a side group. Because of steric reasons and a higher conformational flexibility for the latter case there, the interaction of the phenyl ring of POSS with the phenyl ring of PS might be stronger than for PBAC.

4. Conclusion

Nanocomposites were prepared by blending polyhedral oligomeric silsesquioxane with phenethyl substituents into polystyrene by a well-adapted solution casting method. The evaporation of the solvent was controlled by adjusting the vapor pressure of the solvent in a closed chamber. As a result, homogeneous transparent films are obtained for a reasonable concentration range of PhenethylPOSS from 0 to 40 wt %.

Dielectric spectroscopy shows for polystyrene two relaxation processes indicated by peaks in the dielectric loss. The process at lower frequencies (higher temperatures) is due to the segmental dynamics which is related to the dynamic glass transition (α-relaxation). With increasing concentrations of PhenethylPOSS, the α-relaxation shifts strongly to lower temperatures. Thus, PhenethylPOSS plasticizes the polystyrene matrix. Analyzing the dielectric spectra gives no indication for a further relaxation process or shoulder which would indicate a phase separated morphology. So it is concluded that PhenethylPOSS is miscible into polystyrene up to at least 40 wt %. Adding 40 wt % shifts the glass transition temperature by 50 K to lower temperatures. This is less than expected from the Fox equation which is believed to be valid for a system which is miscible on a molecular level where no extra effects are taking place. Also the density of the nanocomposites is higher than predicted for a simple additive system. It is assumed that

attractive interactions occur in the nanocomposites which increase the density and slow down the molecular dynamics in comparison to a simple additive behavior without any preferential interaction of both the constituents. This line of argumentation is further supported by an analysis of the temperature dependence of the dielectric relaxation strength. This analysis yields to the conclusion that the Kirkwood−Fröhlich interaction parameter g which describes static correleations between molecules is quite different for polystyrene and the nanocomposites with a rather low content of PhenethylPOSS. It is discussed that interactions occur between the phenyl rings of the polystyrene matrix and that of PhenethylPOSS. Probably these interactions are the molecular reasons that PhenethylPOSS is miscible in polystyrene up to quite high concentrations.

PhenethylPOSS/polycarbonate nanocomposites have a phase-separated morphology for higher concentrations of POSS. When compared to polystyrene for polycarbonate, the phenyl ring is located in the polymer backbone. Because of steric reasons, there are less interaction possibilities of the phenyl rings of POSS with those of the polymer than for polystyrene.

The loss peak broadens with increasing concentration. In the framework of the relaxation time spectra, this points to more heterogeneous molecular fluctuations. Therefore the broadening of the loss peak with increasing concentration of POSS is interpreted by composition fluctuations on the scale of a few nanometers.

Acknowledgment. The authors gratefully acknowledge our colleagues in Federal Institute of Materials Research and Testing (BAM), Dr. J. Falkenhagen, Dipl.-Phys O. Hölck, D. Neubert, and K. Brademann-Jock for their assistance. The financial support from the PhD program of BAM (N. Hao) is highly appreciated.

References and Notes

(1) Novak, B. M. *Adv. Mater.* **1993**, *5*, 422.
(2) Vaia, R. A.; Giannelis, E. P. *MRS Bull.* **2001**, *26*, 394.
(3) Krishnamoorti, R., Vaia, R. A., Eds. *Polymer Nanocomposites: Synthesis, Characterization, and Modeling*; ACS Symposium Series 804; American Chemical Society: Washington, DC, 2002.
(4) Mackay, M. E.; Dao, T. T.; Tuteja, A.; Ho, D. L.; Van Horn, B.; Kim, H. C.; Hawker, C. J. *Nat. Mater.* **2003**, *2*, 762.
(5) Merkel, T. C.; Freeman, B. D.; Spontak, R. J.; He, Z.; Pinnau, I.; Meakin, P.; Hill, A. J. *Science* **2002**, *296*, 519. Merkel T. C.; He, Z.; Pinnau, I.; Freeman, B. D.; Meakin, P.; Hill, A. J. *Macromolecules* **2003**, *36*, 6844.
(6) Heilmann, A. *Polymer Films with Embedded Metal Nanoparticles*; Springer: Berlin, Germany, 2003.
(7) Xie, X. L.; Mai, Y. W.; Zhou, X. P. *Mater. Sci. Eng. Res.* **2005**, *49*, 89.
(8) POSS and PhenethylPOSS are trademarks for Polyhedral Oligomeric Silsesquioxane and phenethyl-silsesquioxane (MS0870) of Hybrid Plastics Inc. (Hattiesburg, MS,), respectively. See also www.hybrid-plastics.com
(9) Lichtenhan, J. D.; Schwab, J. J.; Reinerth, W. A. *Chem. Innovation* **2001**, *31*, 3.
(10) Joshi, M.; Butola, B. S. *J. Macromol. Sci., Polym. Rev.* **2004**, *C44*, 389.
(11) Zhao, Y. Q.; Schiraldi, D. A. *Polymer* **2005**, *46*, 11640.
(12) Hao, N.; Böhning, M.; Goering, H.; Schönhals, A. *Macromolecules* **2007**, *40*, 2955.
(13) Phillips, S. H.; Haddad, T. S.; Tomczak, S. J. *Curr. Opin. Solid State Mater. Sci.* **2004**, *8*, 21.
(14) Haddad, T. S.; Lichtenhan, J. D. *J. Inorg. Organomet. Polym.* **1995**, *5*, 237.
(15) Fina, A.; Abbenhuis, H. C. L.; Tabuani, D.; Camino, G. *Polym. Degrad. Stab.* **2006**, *91*, 2275.
(16) Fina, A.; Abbenhuis, H. C. L.; Tabuani, D.; Frache, A.; Camino, G. *Polym. Degrad. Stab.* **2006**, *91*, 1064.
(17) Fina, A.; Tabuani, D.; Frache, A.; Camino, G. *Polymer* **2005**, *46*, 7855.
(18) Fu, B. X.; Yang, L.; Somani, R. H.; Zong, S. X.; Hsiao, B. S.; Phillips, S.; Blanski, R.; Ruth, P. *J. Polym. Sci., Polym. Phys.* **2001**, *39*, 2727.
(19) Pracella, M.; Chionna, D.; Fina, A.; Tabuani, D.; Frache, A.; Camino, G. *Macromol. Symp.* **2006**, *234*, 59.
(20) Joshi, A.; Butola, B. S. *Polymer* **2004**, *45*, 4953.
(21) Joshi, M.; Butola, B. S.; Simon, G.; Kukaleva, N. *Macromolecules* **2006**, *39*, 1839.
(22) Kopesky, E. T.; Boyes, S. G.; Treat, N.; Cohen, R. E.; McKinley, G. H. *Rheol. Acta* **2006**, *45*, 971.
(23) Kopesky, E. T.; McKinley, G. H.; Cohen, R. E. *Polymer* **2006**, *47*, 299.
(24) Kopesky, E. T.; Haddad, T. S.; McKinley, G. H.; Cohen, R. E. *Polymer* **2005**, *46*, 4743.
(25) Kopesky, E. T.; Haddad, T. S.; Cohen, R. E.; McKinley, G. H. *Macromolecules* **2004**, *37*, 8992.
(26) Soong, S. Y.; Cohen, R. E.; Boyce, M. C.; Mulliken, A. D. *Macromolecules* **2006**, *39*, 2900.
(27) Soong, S. Y.; Cohen, R. E.; Boyce, M. C. *Polymer* **2007**, *48*, 1410.
(28) Schiraldi, D.; Iyer, S.; Somlai, A. P.; Zeng, J. J.; Kumar, S.; Bennett, C.; Jarrett, W. L.; Mathias, L. J. *PMSE* [*Prepr*]. **2004**, *227*, U473.
(29) Schiraldi, D.; Zeng, J. J.; Kumar, S.; Iyer, S.; Dong, F. *PMSE* [*Prepr*]-. **2003**, *225*, U59.
(30) Zeng, J.; Kumar, S.; Iyer, S.; Schiraldi, D. A.; Gonzalez, R. I. *High Perform. Polym.* **2005**, *17*, 403.
(31) Kim, K. M. *Polym.-Korea* **2006**, *30*, 380.
(32) Hosaka, N.; Torikai, N.; Otsuka, H.; Takahara, A. *Langmuir* **2007**, *23*, 902.
(33) Blanski, R. L.; Phillips, S. H.; Lee, A. *PMSE* [*Prepr*]. **2001**, *221*, U334.
(34) Blanski, R. L.; Phillips, S. H.; Chaffee, K.; Lichtenhan, J.; Lee, A.; Geng, H. P. *PMSE* [*Prepr*]. **2000**, *219*, U413.
(35) Li, G. Z.; Wang, L.; Toghiani, H.; Daulton, T. L.; Pittman, C. U. *Polymer* **2002**, *43*, 4167.
(36) Pracella, M.; Chionna, D.; Fina, A.; Tabuani, D.; Frache, A.; Camino, G. *Macromol. Symp.* **2006**, *234*, 59.
(37) Blanski, R. L.; Phillips, S. H.; Chaffee, K.; Lichtenhan, J.; Lee, A.; Geng H. P. *Mater. Res. Soc. Symp. Proc.* **2000**, *628*, CC6.27.1.
(38) Hao, N.; Böhning, M.; Schönhals, A. *PMSE* [*Prepr*]. **2007**, *97*, 444.
(39) Schönhals, A. Molecular Dynamics in Polymer Model Systems. In: *Broadband Dielectric Spectroscopy*; Kremer, F., Schönhals, A., Eds.; Springer: Berlin, Germany, 2002; p 225.
(40) Kremer, F.; Schönhals, A. Broadband Dielectric Measurement Techniques. In: *Broadband Dielectric Spectroscopy*; Kremer, F., Schönhals, A., Eds.; Springer: Berlin, Germany, 2002; p 35.
(41) Dechant, J. *Ultrarotspektroskopische Untersuchungen an Polymeren*; Akademie-Verlag: Berlinn, Germany, 1972.
(42) Huang, X. B.; Ouyang, X. Y.; Ning, F. L.; Wang, J. Q. *Polym. Degrad. Stab.* **2006**, *91*, 606.
(43) Lupascu, V.; Picken, S. J.; Wübbenhorst, M. *Macromolecules* **2006**, *39*, 5152.
(44) Lupascu, V.; Picken, S. J.; Wübbenhorst, M. *J. Non-Cryst. Solids* **2006**, *352*, 5594.
(45) McCrum, N. G.; Read, B. E.; Williams, G. Anelastic and Dielectric Effects. In *Polymeric Solids*; Wiley: New York, 1967 (reprinted by Dover Publications, 1991).
(46) Pratt, G. J.; Smith, M. J. A. *Polym. Int.* **1997**, *43*, 137.
(47) Hardy, L.; Fritz, A.; Stevenson, I.; Boiteux, G.; Seytre, G.; Schönhals, A. *Polymer* **2003**, *44*, 4311.
(48) Fritz, A.; Schönhals, A.; Sapich, B.; Stumpe, J. *Makromol. Chem.* **1999**, *200*, 2213.
(49) Turky, G.; Schönhals, A. *Polymer* **2004**, *45*, 255.
(50) Havriliak, S.; Negami, S. *Polymer* **1967**, *8*, 161. Havriliak, S.; Negami, S. *J. Polym. Sci., Part C* **1966**, *16*, 99.
(51) Schönhals, A.; Kremer, F. Analysis of Dielectric Spectra. In *Broadband Dielectric Spectroscopy*; Kremer, F., Schönhals, A. Eds.; Springer: Berlin, Germany, 2002; p 59.
(52) Vogel, H. *Phys. Z.* **1921**, *22*, 645. Fulcher, G. S. *J. Am. Ceram. Soc.* **1925**, *8*, 339. Tammann, G.; Hesse, W. *Z. Anorg. Allg. Chem.* **1926**, *156*, 245.
(53) Kremer, F.; Schönhals, A. The Scaling of the Dynamics of Glasses and Supercooled Liquids Spectra. In *Broadband Dielectric Spectroscopy*; Kremer, F., Schönhals, A., Eds.; Springer: Berlin, Germany, 2002; p 99.
(54) Schönhals, A.; Kremer, F. Theory of Dielectric Relaxation Spectra in Broadband Dielectric Spectroscopy; In *Broadband Dielectric Spectroscopy*; Kremer, F., Schönhals, A., Eds.; Springer: Berlin, Germany, 2002; p 1.
(55) Yada, M.; Nakazawa, M.; Urakawa, O.; Morishima, Y.; Adachi, K. *Macromolecules* **2000**, *33*, 3368.
(56) Nakazawa, M.; Urakawa, O.; Adachi, K. *Macromolecules* **2000**, *33*, 7898.
(57) Katana, G.; Fischer, E. W.; Hack, T.; Abetz, V.; Kremer, F. *Macromolecules* **1995**, *28*, 2714.
(58) Fischer, E. W.; Zetsche, A. *Abstr. Pap. Am. Chem. Soc.* **1992**, *33*, 78.
(59) Donth, E. *The Glass Transition*; Springer-Verlag: Berlin, Germany, 2001.
(60) Kivelson, D.; Kivelson, S. A.; Zhao, X.; Nussinov, Z.; Tarjus, G. *Physica* **1995**, *A219*, 27.

MA071777G